Astron. Astrophys. 364, 249–264 (2000)

ASTRONOMY
AND
ASTROPHYSICS

Barium and europium abundances in cool dwarf stars and nucleosynthesis of heavy elements⋆

L. Mashonkina[1,2,3] **and T. Gehren**[2]

[1] Department of Astronomy, Kazan State University, Kremlevskaya 18, Kazan 8, Russia, 420008
[2] Institut für Astronomie und Astrophysik der Universität München, Scheinerstrasse 1, 81679 München, Germany
[3] Max-Planck-Institut für Astrophysik, Karl-Schwarzschild-Strasse 1, 85740 Garching, Germany

Received 25 May 2000 / Accepted 14 September 2000

Abstract. We revise barium abundances in 29 cool stars with metallicities [Fe/H] ranging from -2.20 to 0.07 and europium abundances in 15 stars with [Fe/H] from -1.52 to 0.07. The sample has been extracted from Fuhrmann's lists (1998, 2000) and confined to main-sequence and turnoff stars with only one subgiant added. The results are based on differential NLTE model atmosphere analyses of spectra that have a typical S/N of 200 and a resolution of 40000 or 60000. The statistical equilibrium of Eu II is first investigated with a model atom containing 32 levels of Eu II plus the ground state of Eu III. NLTE effects decrease the equivalent widths of the Eu II lines compared with LTE resulting in positive NLTE abundance corrections which are below 0.08 dex for all the stars investigated. The solar barium abundance $\log \varepsilon_{\rm Ba,\odot} = 2.21$ and the europium abundance $\log \varepsilon_{\rm Eu,\odot} = 0.53$ are found from the Ba II and Eu II solar flux line profile fitting, and they coincide within error bars with meteoritic abundances of Grevesse et al. (1996). Here the usual scale with $\log \varepsilon_{\rm H} = 12$ is used. The isotopic ratio ^{151}Eu: ^{153}Eu = 55: 45 is obtained from solar disk center intensity profile fitting of the Eu II λ4129 Å line. We report here for the first time that the elemental ratios [Ba/Fe], [Eu/Fe] and [Eu/Ba] show a different behaviour for stars of different Galactic populations. For the halo stars the [Ba/Fe] ratios are approximately solar, europium is overabundant relative to iron and barium with the mean values [Eu/Fe] = 0.62 and [Eu/Ba] = 0.64. For thick disk stars it is found that a) barium is slightly underabundant relative to iron by about 0.1 dex; b) europium is overabundant relative to iron with the [Eu/Fe] ratios between 0.30 and 0.44; and c) europium is overabundant relative to barium with a mean value of [Eu/Ba] = 0.49 $\pm$ 0.03. A step-like change in the [Eu/Ba] and [Ba/Fe] ratios occurs at the thick to thin disk transition; so, nearly solar elemental ratios [Ba/Fe], [Eu/Fe] and [Eu/Ba] are found for the thin disk stars. These data suggest that a) the halo and thick disk stellar population formed quickly during an interval comparable with the evolution time of an AGB progenitor of 3 to 4 $M_\odot$, and the r-process dominated heavy element production at that epoch; b) there was a hiatus in star formation before the early stage of the thin disk developed. The even-to-odd Ba isotope ratios estimated from hyperfine structure (HFS) affecting the Ba II resonance line in the halo and thick disk stars favour a significant contribution of ^{138}Ba to barium for a pure r-process, and this is supported by the recent data of Arlandini et al. (1999).

Key words: line: formation – nuclear reactions, nucleosynthesis, abundances – Sun: abundances – stars: abundances – stars: late-type – Galaxy: evolution

1. Introduction

Formation of elements with $Z > 26$ is commonly believed to result from stellar nucleosynthesis, and to explain the presence of heavy elements in the oldest stars of the Galaxy the idea is suggested that the first stellar generation consisted mostly of high-mass stars. At the end of their short evolution massive stars exploded as type II supernovae (SNII) and enriched the Galactic interstellar gas. Overabundances of α-elements relative to iron observed in old stars argue in favour of this model (see the review of McWilliam 1997). Another argument can be obtained from observations of the heavy elements beyond the iron group. Abundances of these elements in the solar system have contributions in differing proportions from two main processes, the s- and r-process of neutron capture. As supported by many observational and theoretical results (Travaglio et al. 1999, and references therein) s-nuclei are mainly synthesized during the thermally pulsing asymptotic giant branch phase of low-mass stars (2–4 $M_\odot$). The r-process is associated with explosive conditions in SNeII (Freiburghaus et al. 1999, and references therein). If at early times only high-mass stars existed, heavy elements must have been produced by the r-process, and elemental abundances observed in old stars should correspond to the r-process element pattern. The europium to barium abundance ratio is particularly sensitive to whether nucleosynthesis of the heavy elements occured by the s- or r-process. For the solar system matter $\log \varepsilon_{\rm Eu,\odot} - \log \varepsilon_{\rm Ba,\odot} = -1.67$ (Grevesse et al. 1996). The contributions of the s- and r-process to the solar

Send offprint requests to: L. Mashonkina (Lyudmila.Mashonkina@ksu.ru)

⋆ Based on observations at the German Spanish Astronomical Center, Calar Alto, Spain

Ba abundance consist of 88% and 12%, respectively, according to Cameron (1982), 87% and 13% according to Käppeler et al. (1989), and 81% and 19% according to the most recent data of Arlandini et al. (1999). The solar europium mostly originated from the r-process: 91% according to Cameron (1982) and Wisshak et al. (1996). Thus we can compute the solar abundance ratio of Eu to Ba contributed by the r-process, $(\mathrm{Eu/Ba})_r$. Relative to the total abundances the fraction $\log\{(\mathrm{Eu/Ba})_r/(\mathrm{Eu/Ba})\}$ ranges from 0.70 (Arlandini et al. 1999) to 0.89 (Cameron 1982).

Truran (1981) first proposed that the heavy elements in the halo stars are of the r-process origin. Much observational efforts were invested in testing this idea. For extremely metal-poor stars with metallicities [Fe/H] ≤ -2.4 McWilliam (1998) has derived an average [Eu/Ba] = 0.69, consistent with pure r-process nucleosynthesis provided that the data of Arlandini et al. (1999) are adopted. Sneden et al. (1996) have analyzed the very metal-poor star CS22892-052 ([Fe/H] = -3.1) that reveals a heavy element pattern identical to the r-process pattern in the solar system. However, the recent studies of Gratton & Sneden (1994), Francois (1996), Jehin et al. (1999), and Woolf et al. (1995) show a gradual increase in the [Eu/Ba] ratio from 0 up to about 0.7 with [Fe/H] decreasing from 0 to -2.

Estimating Ba and Eu abundances and their ratios in metal-poor stars is one of the aims of this study, and we show that there is a clear separation between stars with an overabundance of Eu relative to Ba and stars with Eu/Ba ratios close to solar. This separation is defined not so much by metallicity as by membership in a particular stellar population of the Galaxy. All the halo and thick disk stars of our sample with [Fe/H] from -0.34 to -1.5 show high values of [Eu/Ba] with only small scatter that indicates r-process dominated nucleosynthesis at times of formation not only of the halo but also of the thick disk stellar population.

The fraction of the s- and r-process in producing heavy elements can be evaluated by another method, from an analysis of the hyperfine structure (HFS) affecting the Ba II $\lambda 4554$ line. The idea is based on the fact that the larger the r-process contribution is, the larger the fraction of odd isotopes must be, and the greater the HFS broadening of this line. For the extremely metal-poor star HD 140283 Magain & Zhao (1993) and Magain (1995) have found from a measurement of the broadening of this line an isotopic composition close to solar. In our previous paper (Mashonkina et al. 1999, thereafter Paper I) we suggested a different method based on an estimation of the Ba abundance from the subordinate lines that are free of HFS effects. Simultaneously, we were able to evaluate the even-to-odd Ba isotope ratio from measuring the total energy absorbed in the resonance line. From analyses of the halo stars with [Fe/H] = -1.5 and -2.2 we have concluded that these stars were formed from matter with barium produced by both s- and r-processes at an r/s-process ratio close to solar. So, conclusions drawn from analysis of the Ba II resonance line seem to contradict the above mentioned results derived from the [Eu/Ba] ratios. However it is important to note that from a study of HFS affecting the Ba II $\lambda 4554$ line we obtain the ratio of odd to even Ba isotopes and then deduce the r/s-process ratio on the base of given r- and s-process contributions to each isotope. Magain & Zhao (1993), Magain (1995) and Paper I results are based on the data of Cameron (1982) who gives the ratio of even to odd Ba isotopes ^{138}Ba: (^{135}Ba + ^{137}Ba) = 28: 72 for a pure r-process. As ^{135}Ba and ^{137}Ba, responsible for HFS components, contain a majority of barium the Ba II $\lambda 4554$ line is significantly strengthened compared with the case of solar even-to-odd isotopic ratio 82: 18. In Paper I we showed this difference can be easily detected if it exists: for example, for the star BD 66°268 with [Fe/H] = -2.2 it consists of 0.2 dex in terms of abundances. However at Ba abundances derived from the Ba II subordinate lines we could not find a marked strengthening of the Ba II resonance line in spectra of both normal metallicity and metal-poor stars. Wisshak et al. (1996) note that the ratio ^{138}Ba: (^{135}Ba + ^{137}Ba) for pure r-process is very difficult to determine, as the r-process abundance of ^{138}Ba is very small and calculated as the difference of solar and s-process abundances. This is the difference of two large numbers and correspondingly has a very large uncertainty. They give the ^{138}Ba isotope abundance for a pure r-process as 28% with uncertainty up to 110%. The most recent measurements of Arlandini et al. (1999) have improved this value and increased it up to 54%.

This study is aimed to derive odd-to-even Ba isotope ratios for the stars revealing an overabundance of Eu relative to Ba and estimate an acceptable range of the r/s-process ratio using the data of Arlandini et al. (1999).

Our sample includes 29 stars from Fuhrmann's (1998, 2000) lists with effective temperatures $T_{\rm eff}$ from 5110 K to 6500 K, surface gravities $\log g$ from 4.0 to 4.66 except for HD 45282 with $\log g$ = 3.12 and HD 117176 with $\log g$ = 3.83, and metallicities [Fe/H] between 0.07 and -2.20. Only main sequence stars (MS) or stars close to the MS are selected to make sure that atmospheric abundances reflect the real chemical composition of interstellar matter out of which the star was formed and to reduce methodical errors connected with the determination of fundamental parameters and modeling of giant stellar atmospheres. Stellar parameters $T_{\rm eff}$, $\log g$, [Fe/H] and microturbulence $V_{\rm mic}$ carefully estimated by Fuhrmann (1998, 2000) are believed to be of high accuracy. As in Paper I elemental abundances are derived from line profile fitting and not from equivalent widths W_λ. A differential analysis with respect to the Sun is used which means that oscillator strengths f_{ij} and van der Waals damping constants C_6 were determined in advance from solar line profile fitting. Non-local thermodynamical equilibrium (NLTE) line formation is considered to obtain theoretical Ba II and Eu II line profiles. The method of NLTE calculations for Ba II was developed earlier (Paper I). The statistical equilibrium of Eu II is studied for the first time.

Use of high-resolution spectra (R = 40000 and 60000), reliable stellar parameters and line formation astrophysics has made it possible to improve stellar Ba and Eu abundances and to detect the important trends in the behaviour of elemental ratios [Ba/Fe], [Eu/Fe] and [Ba/Eu].

This paper is organized as follows. Observations and stellar parameters are shortly described in Sect. 2. The Eu II model atom and NLTE effects for Eu II are presented in Sect. 3. In

the next section solar Ba II and Eu II line profiles are fitted to improve empirically their atomic parameters and to deduce solar Ba and Eu abundances and ^{151}Eu: ^{153}Eu isotopic ratio. In Sect. 5 we present and discuss the results obtained, stellar Ba and Eu abundances and their ratios and estimates of the odd to even Ba isotope ratios. Final conclusions are given in Sect. 6.

2. Observations and stellar parameters

Our results are based on spectra observed by Klaus Fuhrmann, Michael Pfeiffer and Andreas Korn using the fiber optics Cassegrain échelle spectrograph FOCES fed by the 2.2m telescope at the Calar Alto observatory during 4 observing runs in September 1995, May 1997, December 1998 - January 1999 and in June 1999. The data cover an approximate spectral range of 4000–7000 Å. The 1995 spectra were exposed to a 1024×1024 24μ CCD, and the resolving power was $\sim$ 40000. Starting from May 1997 a 2048×2048 $15\,\mu$ CCD was employed at $\lambda/\Delta\lambda$ $\sim$60000. Almost all the stars were observed at least twice with the signal-to-noise ratio of about 200 (Fuhrmann 1998, 2000) in the spectral range $\lambda \geq 4550$ Åand with less S/N ($\sim$ 50) in the range where the Eu II resonance line λ4129 is located. Our sample of 9 stars from Paper I with metallicities [Fe/H] mostly lower than -1 was extended in this study by including 3 halo stars and 17 stars with [Fe/H] between 0 and -1. Ba abundances obtained in Paper I are revised using the advanced NLTE method (Sect. 4.1) and the stellar parameters adopted in this work. Stellar parameters taken in Paper I differ from those used in this study by 150 K for $T_{\rm eff}$ and by 0.1 dex for $\log g$ at maximum. In fact, it has negligible effect on elemental ratios [Ba II/Fe II], however, we prefer to use for all the stars of our sample parameters determined by the same methods. Table 1 lists the stars selected.

We use spectra reduced according to the description given in Pfeiffer et al. (1998). The instrumental profile is found from comparison of FOCES Moon spectra with the Kitt Peak Solar Flux Atlas (Kurucz et al. 1984). A Gaussian of 4.6 ± 0.2 km s^{-1}provides the best fit to the September 1995 spectra (Fuhrmann et al. 1997), and 3.2 km s^{-1}, 3.6 km s^{-1}and 4.9 km s^{-1}are appropriate for the May 1997, December 1998 - January 1999 and June 1999 observations correspondingly (Fuhrmann 1998, 2000).

For most of the stars stellar parameters determined spectroscopically are taken from the careful analyses of Fuhrmann (1998, 2000). Effective temperatures have been deduced from Balmer line profile fitting and surface gravities $\log g$ from line wings of the Mg Ib triplet. Metallicities [Fe/H] and microturbulence values $V_{\rm mic}$ have been derived from the Fe II line profile fitting. For three stars the stellar parameters have been estimated by Frank Grupp (1997: BD 66°268 and BD 29°366) and Andreas Korn (1999: BD 34°2476) using the same methods. All the parameters are given in Table 1. The identification of stellar population for all stars of our sample is from Fuhrmann (1998, 2000), based on the star's kinematics, α-element enhancement and age, and we give this important information for our study in Table 1, too.

Table 1. Stellar parameters of the selected sample. Most of the entries are self-explanatory. In Column 8 the notations refer to the thin disk, thick disk and halo stars, respectively. $V_{\rm mic}$ is given in km s^{-1}

HD/BD	$T_{\rm eff}$ [K]	$\log g$	[Fe/H]	$V_{\rm mic}$	[Ba/Fe]	[Eu/Fe]	Note
1	2	3	4	5	6	7	8
400	6150	4.06	–0.25	1.3	0.02	0.12	thin
6582	5390	4.45	–0.83	0.9	–0.10:	0.33:	thick
9407	5660	4.42	0.03	0.9	–0.09	–	thin
19445	6020	4.38	–1.95	1.4	–0.08	–	halo
22879	5870	4.27	–0.86	1.2	–0.03	–	thick
30649	5820	4.28	–0.47	1.2	–0.10	0.40	thick
43042	6440	4.23	0.04	1.5	–0.01	–	thin
45282	5280	3.12	–1.52	1.4	–0.04	0.62	halo
52711	5890	4.31	–0.16	1.0	0.01	–	thin
61421	6500	4.04	0.00	1.9	–0.14	0.02	thin
62301	5940	4.06	–0.69	1.3	–0.05	–	thick
69611	5820	4.18	–0.60	1.2	–0.09	0.38	thick
84937	6350	4.03	–2.07	1.7	0.01	–	halo
102158	5760	4.24	–0.46	1.1	–0.13	0.39	thick
103095	5110	4.66	–1.35	0.8	0.04	–	halo
114762	5930	4.11	–0.71	1.2	–0.12	–	thick
117176	5480	3.83	–0.11	1.0	–0.06	–	thin
157214	5735	4.24	–0.34	1.0	–0.13	0.30	thick
184499	5830	4.13	–0.51	1.2	–0.16	0.34	thick
186408	5800	4.26	0.06	1.0	–0.03	–	thin
187691	6090	4.07	0.07	1.4	–0.09	-0.01	thin
194598	6060	4.27	–1.12	1.4	0.00:	0.61:	halo
201891	5940	4.24	–1.05	1.2	–0.07:	0.41	thick
204155	5830	4.12	–0.63	1.2	–0.18	0.33:	thick
221830	5750	4.19	–0.36	1.2	–0.04	0.44	thick
2°3375	6140	4.31	–2.15	1.4	–0.13	–	halo
29°366	5740	4.60	–0.93	1.3	–0.08	0.43	?
34°2476	6330	4.03	–1.96	1.8	0.09	–	halo
66°268	5340	4.60	–2.20	0.9	0.07	–	halo

Fuhrmann (1998) estimates a typical uncertainty $\Delta T_{\rm eff}$ = 80 K which translates to an abundance error up to 0.05 dex for elemental abundances deduced from spectral lines of the dominant ionization stages such as Ba II, Eu II, Fe II. From a comparison with the accurate HIPPARCOS distances Fuhrmann (1998) finds that his spectroscopic distance scale is only slightly higher, by 3.4% on average, and the statistical *rms* error is 5%. The systematic deviation of 3.4% translates to a $\Delta \log g$ of only 0.03 dex and to a $\Delta \log \varepsilon$ of about 0.01 dex in the cases of Ba II, Eu II and Fe II. Fuhrmann (1998) estimates carefully the precision in $\log g$ of ~ 0.1 dex which propagates into 0.04 dex in abundances. However, elemental ratios [Ba II/Fe II], [Eu II/Fe II] and [Eu II/Ba II] are expected to be much less affected by possible errors of $T_{\rm eff}$ and $\log g$. And an uncertainty of $V_{\rm mic}$ turns out to have the largest effect on the abundance ratios [Ba II/Fe II] and [Eu II/Ba II]. Only relatively weak Fe II lines were selected by Fuhrmann (1998, 2000) to derive stellar iron abundances. Eu abundances are found in this study from the Eu II $\lambda4129$ and $\lambda6645$ lines with equivalent widths below 55 mÅ and 6 mÅ. Thus, an uncertainty of $V_{\rm mic} = 0.2$ km s^{-1} given by Fuhrmann

(1998) has negligible effect (up to 0.005 dex) on [Fe/H] and [Eu/H]. In the case of barium we are forced to use the Ba II lines lying on the flat part of the curve of growth. For the stars with [Fe/H] > -0.7 $V_{\rm mic} = 0.2$ km s^{-1} propagates into $\Delta \log \varepsilon_{\rm Ba} \simeq 0.1$ dex even when using the weakest subordinate line Ba II $\lambda5853$. For the most metal-poor stars of our sample where the resonance Ba II $\lambda4554$ line is used, $V_{\rm mic} = 0.2$ km s^{-1}gives $\Delta \log \varepsilon_{\rm Ba} = 0.12$ dex.

In total, uncertainties of stellar parameters cause abundance errors up to $\Delta \log \varepsilon_{\rm Ba} = 0.11$ dex and $\Delta \log \varepsilon_{\rm Eu} = 0.05$ dex for the stars with [Fe/H] ≥ -0.5, up to $\Delta \log \varepsilon_{\rm Ba} = 0.08$ dex and $\Delta \log \varepsilon_{\rm Eu} = 0.06$ dex in the range of metallicities between -0.5 and -1.5 and for the most metal-poor stars Ba abundance error can reach to 0.14 dex. Errors of elemental ratios are smaller and can be obtained from the values given.

Our analyses are all based on the same type of model, irrespective of temperature, gravity or metal abundance. We used line-blanketed LTE model atmospheres generated and discussed by Fuhrmann et al. (1997).

3. NLTE calculations for Eu II

3.1. Model atom

NLTE calculations for Eu II were performed for the first time by one of us (Mashonkina 2000). We use the same method with some modifications concerning collisional rate computations. We describe briefly the new results.

The Eu II model atom has a complex term structure including nonet, septet, quintet levels etc. Laboratory measurements (Martin et al. 1978) give 88 energy levels for 25 nonet and septet terms of the $4f^7$ nl and $4f^6 5d$ nl′ electronic configuration. For another 83 energy levels with energy excitation above 4 eV only the total angular momentum and the parity are known. We include into the Eu II model atom all the measured nonet and septet terms and radiatively couple to them the levels of unknown configurations. For NLTE calculations only the level energy and oscillator strengths f_{ij} of transitions connecting that level with others are important. So, assuming that the measured energy levels of unknown configurations belong to nonet or septet terms we have composed 6 septet terms and 5 nonet terms. They are marked by "?" in Fig. 1. Remaining levels of unknown configurations are taken into account only for number conservation. Levels with the small energy differences were combined into single level. The fine structure is in part considered only for the $5d\,^9{\rm D}^\circ$ and $6p\,^9{\rm P}$ terms that concern the transitions of our special interest: $6s\,^9{\rm S}^\circ_4 - 6p\,^9{\rm P}_4$ forming the Eu II resonance line $\lambda4129$ Å and $5d\,^9{\rm D}^\circ_6 - 6p\,^9{\rm P}_5$ for $\lambda6645$ Å. Thus, 32 bound levels of Eu II and the ground state of Eu III are included into the model atom. The corresponding Grotrian diagram is shown in Fig. 1. In Table 2 for every term the energy levels combined and the average ionization frequencies, ν_{ion}, are given. Photoionization of the $4f^6 5d$ nl′ levels connects to the excited Eu III $4f^6 5d$ levels. Five octet and 5 sextet Eu III $4f^6 5d$ terms with excitation energies from measurements of Martin et al. (1978) were combined into 3 energy levels which are assumed to be in thermal equilibrium relative to the Eu III ground state. That is why in Table 2 three

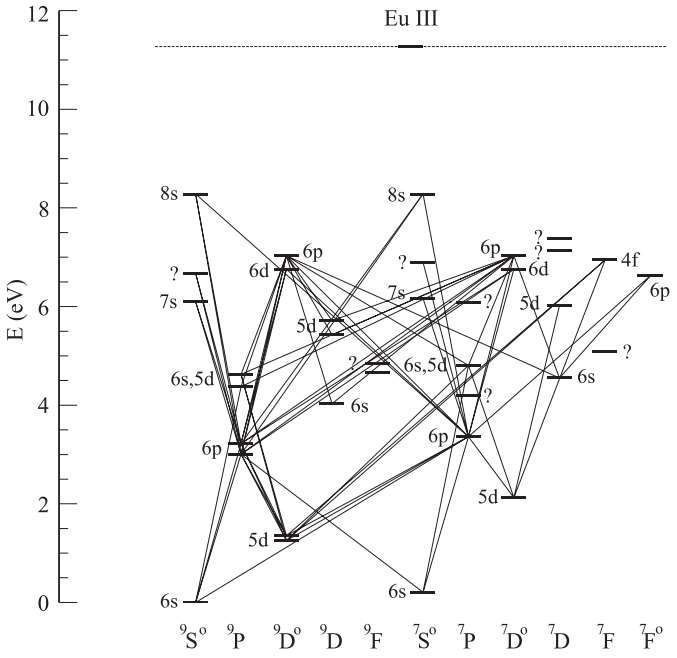

Fig. 1. The Eu II model atom. The linearized transitions are shown as solid lines

values of ν_{ion} are given for every nl′ level. Photoionization of the levels indicated by "?" is considered similarly to the nl′ levels.

The adopted model atom looks incomplete. Missing all quintet, triplet and singlet levels and highly excited nonet and septet levels that have to provide close collisional coupling to the continuum electron reservoir can cast some doubt upon our results. Let us consider this point and start from highly excited levels. In atmospheres of F - G stars Eu III contains a minor fraction of the element; for the Sun $\log n({\rm Eu\,II})/n({\rm Eu\,III}) = 1.5$ in deep layers near $\log \tau_{5000} = 0$, and it grows up to 3.5 in upper atmospheric layers. It means that no processes coupling the Eu II levels to Eu III can significantly affect populations of the low-excitation Eu II terms that contain the major population fraction of the element. And NLTE effects are expected mainly due to radiative bound - bound (b-b) transitions between levels of low excitation. To prove this statement by numerical calculations we have considered an extended Eu II model atom. Based on the fact that the Eu II and Ba II atoms have similar term structure, and that the Eu II and Ba II level energies reveal similar regularities in the behaviour of ionization energy with principal quantum number, we have computed energies of the Eu II $4f^7$ nl levels for n = 7–10 and l = 0–3. In total, we have introduced into the model atom 28 "fake" terms with excitation energies up to 10.5 eV. For transitions including "fake" levels f_{ij} were adopted by analogy with Ba II, too. As expected, the calculations performed with the extended and original model atom show no difference for populations of the important energy levels and intensities of the spectral lines of interest.

Quintets, triplets and singulets do not show up in the laboratory spectrum of Eu II, and this lends support to the assumption that coupling of missing levels to measured ones is weak, and

that such levels can be neglected in statistical equilibrium of Eu II. Their contribution to the Eu II partition function was estimated by Butler (1999) on the base of own computations; in a case of solar-type stars it consists of about 6%. If we neglect missing levels we overestimate populations of the levels included and underestimate Eu abundances deduced from the Eu II lines by about 0.02 - 0.03 dex.

Oscillator strengths are available for all the transitions from the ground state and low excited levels 6s, 5d and 6p to upper levels. The data of Komarovskii (1991) are preferred and, if they are absent, f_{ij} from the compilation of Kurucz (1994) are taken. Missing f_{ij} have been treated as follows: for transitions between double excited levels $4f^6 5d$ nl - $4f^6 5d$ nl′ we adopt f_{ij}-values of the corresponding $4f^7$ nl - $4f^7$ nl′ transitions; for transitions from (or to) "?" levels $f_{ij} = 0.001$ is set.

The photoionization cross-sections for the $6p\,^7\mathrm{P}$ and $6p\,^9\mathrm{P}$ levels have been calculated by the quantum defect method using Peach's (1967) tables. For the remaining levels hydrogenic cross-sections are computed.

For electron impact excitation we use the formula of van Regemorter (1962) for allowed transitions and that of Allen (1973) for forbidden ones. The exception is the forbidden transitions from $6s\,^9\mathrm{S}^\circ$, $6s\,^7\mathrm{S}^\circ$ to $5d\,^9\mathrm{D}^\circ$, $5d\,^7\mathrm{D}^\circ$. Population of the metastable levels depends strongly on collisional coupling to the ground state. Having analysed the results of many test calculations we have adopted finally the formula of van Regemorter for computing collisional rates in $6s\,^9\mathrm{S}^\circ$, $6s\,^7\mathrm{S}^\circ$ - $5d\,^9\mathrm{D}^\circ$, $5d\,^7\mathrm{D}^\circ$ transitions and f_{ij} have been set at one tenth the values for the allowed transitions $6s\,^9\mathrm{S}^\circ$, $6s\,^7\mathrm{S}^\circ$ - $6p\,^9\mathrm{P}$, $6p\,^7\mathrm{P}$. Electron impact ionization cross-sections are computed according to Drawin (1961). For hydrogen collisions, we use the formula of Steenbock & Holweger (1984). Since this formula provides only an order of magnitude estimate, the cross-sections were multiplied by appropriate scaling factors in order to produce the best fit to the solar Eu II level populations and line profiles.

3.2. Statistical equilibrium calculations and NLTE effects

The Eu II statistical equilibrium is calculated using the code NONLTE3 (Sakhibullin 1983) which is based on the complete linearization method as described by Auer & Heasley (1976). The advanced method of calculations has been described in detail in Paper I.

Similarly to Ba II, at $T_{\rm eff}$ and $\log g$ close to solar values the statistical equilibrium of Eu II is strongly affected by radiative processes in b-b transitions. However, in contrast to Ba II, NLTE leads to a weakening of the Eu II lines compared with the LTE case. We consider the mechanisms and the physics behind this for the Sun. For other stars of our sample NLTE effects for Eu II are qualitatively the same. In Fig. 2 the departure coefficients, $b_i = n_i^{\rm NLTE}/n_i^{\rm LTE}$ as a function of continuum optical depth τ_{5000} refering to $\lambda = 5000$ Å are shown for the lowest 8 levels necessary for subsequent line profile synthesis and for understanding the NLTE mechanisms. Here, $n_i^{\rm NLTE}$ and $n_i^{\rm LTE}$ are the statistical equilibrium and thermal (Saha-Boltzmann) number densities, respectively.

Table 2. Eu II model atom

No.	Term	J	ν_{ion} $10^{15}Hz$	No.	Term	J	ν_{ion} $10^{15}Hz$
1	$6s\,^9\mathrm{S}^\circ$	4	2.71807	19	$5d'\,^9\mathrm{D}$	6	2.44105
2	$6s\,^7\mathrm{S}^\circ$	3	2.66803				2.48647
3	$5d\,^9\mathrm{D}^\circ$	2–4	2.41510				2.56623
4	$5d\,^9\mathrm{D}^\circ$	5,6	2.39172	20	$5d'\,^7\mathrm{D}$	1–5	2.36705
5	$5d\,^7\mathrm{D}^\circ$	1–5	2.20496				2.41245
6	$6p\,^9\mathrm{P}$	3,4	1.99884				2.49221
7	$6p\,^9\mathrm{P}$	5	1.93343	21	$?\,^7\mathrm{P}$	2–4	2.35242
8	$6p\,^7\mathrm{P}$	2–4	1.90664				2.39784
9	$6s'\,^9\mathrm{D}$	2–6	2.84748				2.47759
			2.89289	22	$7s\,^9\mathrm{S}^\circ$	4	1.24525
			2.97265	23	$7s\,^7\mathrm{S}^\circ$	3	1.22970
10	$?\,^7\mathrm{P}$	2–4	2.80523	24	$6p'\,^7\mathrm{F}^\circ$	0–6	2.22109
	$6s'\,^9\mathrm{P}$	3–5	2.85065				2.26650
			2.93041				2.34626
11	$?\,^9\mathrm{P}$	3,4	2.76485	25	$?\,^9\mathrm{S}^\circ$	4	2.20860
	$?\,^9\mathrm{P}$	3,4	2.81027				2.25401
			2.89003				2.33377
12	$6s'\,^7\mathrm{D}$	1–5	2.72148	26	$6d\,^9\mathrm{D}^\circ$	2–6	1.08641
			2.76689		$6d\,^7\mathrm{D}^\circ$	1–5	
			2.84665	27	$?\,^7\mathrm{S}^\circ$	3	2.15535
13	$5d'\,^9\mathrm{P}$	3–5	2.70473				2.20077
			2.75015				2.28053
			2.82091	28	$4f\,^7\mathrm{F}$	0–6	1.04102
14	$?\,^9\mathrm{F}$	2–6	2.69526	29	$6p'\,^7\mathrm{D}^\circ$	1–5	2.12412
			2.74068		$6p'\,^9\mathrm{D}^\circ$	2–5	2.16954
			2.82044				2.24930
15	$6s'\,^7\mathrm{P}$	2–4	2.66013	30	$?\,^7\mathrm{D}$	1–4	2.09865
	$5d'\,^7\mathrm{P}$	2–4	2.70555				2.14407
			2.78530				2.22382
16	$?\,^9\mathrm{F}$	1–7	2.64940	31	$?\,^7\mathrm{D}$	1–4	2.03856
			2.69482				2.08398
			2.77457				2.16374
17	$?\,^7\mathrm{F}$	4,6	2.59411	32	$8s\,^9\mathrm{S}^\circ$	4	0.71794
	$?\,^7\mathrm{F}$	4–6	2.63953		$8s\,^7\mathrm{S}^\circ$	3	
			2.71928	33	Eu III	7/2	
18	$5d'\,^9\mathrm{D}$	2–5	2.51062				
			2.55604				
			2.63579				

Due to close collisional coupling the metastable level $6s\,^7\mathrm{S}^\circ$ follows the ground state and the fine structure levels of $5d\,^9\mathrm{D}^\circ$ (numbers 3 and 4) show actually the same behaviour, so, we will mention below only the ground state and the term $5d\,^9\mathrm{D}^\circ$. In the line formation layers, outside $\log\tau_{5000}$ = 0.3 the ground state is slightly underpopulated and the excited levels are overpopulated. An enhanced excitation of $6p\,^9\mathrm{P}$ and $6p\,^7\mathrm{P}$ levels is produced by the pumping transitions $6s\,^9\mathrm{S}^\circ$ - $6p\,^9\mathrm{P}$, $6p\,^7\mathrm{P}$ and $6s\,^7\mathrm{S}^\circ$ - $6p\,^9\mathrm{P}$, $^7\mathrm{P}$. The terms $5d\,^9\mathrm{D}^\circ$ and $5d\,^7\mathrm{D}^\circ$ are overpopulated relatively to the ground state by filling up from $6p\,^9\mathrm{P}$ and $6p\,^7\mathrm{P}$ via the line transitions in the layers transparent for the radiation of corresponding wavelengths, at optical depth $\log\tau_{5000} < 0.3$. The excitation energies of $5d\,^9\mathrm{D}^\circ$ and $5d\,^7\mathrm{D}^\circ$ are not so small ($\sim$ 1.1 eV and 1.9 eV) and their coupling to the ground state turns out weaker than a coupling to $6p$ levels and to each other. Roughly speaking, an electron that got to the $6p$ levels from the ground state has a small chance to

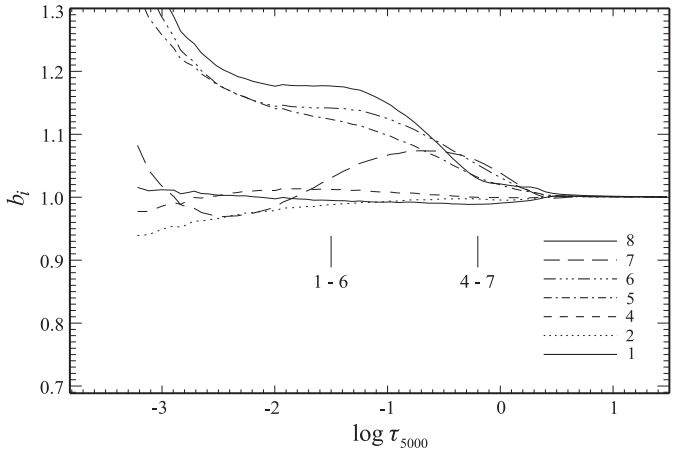

Fig. 2. Departure coefficients b_i for some levels of Eu II in the model atmosphere of the Sun. Numbers near curves correspond to the level numbers in Table 2. Departure coefficients of the third and forth levels are close together and only b_4 is presented. Tick marks indicate the locations of line center optical depth unity for the Eu II lines λ4129 Å (1–6) and λ6645 Å (4–7)

come back because it is easily trapped by the chain of transitions $6p\,^9\mathrm{P} \rightarrow 5d\,^7\mathrm{D}^\circ \rightarrow 6p\,^7\mathrm{P}$ or in opposite direction. An occurence of the pair of $5d$ and the pair of $6p$ terms strongly coupled to each other is a special feature of Eu II in comparison with Ba II and it favours an overpopulation of the $5d$ and $6p$ terms from the ground state electron reservoir in contrary to Ba II where a chain of transitions $6s \rightarrow 6p \rightarrow 5d \rightarrow 6s$ results in an underpopulation of $6p$ (Paper I). By analogy with Ba II, the Eu II levels above $6p\,^7\mathrm{P}$ are overpopulated by pumping transitions arising from the $6p$ terms. The continuum is overpopulated, too, because of its radiative and collisional coupling to the upper levels. From this behaviour of departure coefficients we expect that our Eu II lines of interest are weakened compared with the LTE case, because for both of them $b_u/b_l > 1$ is valid in line formation layers resulting in a source function S_{lu} greater than $B_\nu(T_e)$. An underpopulation of the ground state is added to weaken the resonance line λ4129. For the subordinate line λ6645 an enhanced excitation of the lower level (number 4 in Fig. 2) competes with the first factor, $S_{lu} > B_\nu(T_e)$, resulting in small NLTE effects for this line.

We summarize, departures from LTE for the Eu II lines are not very large. NLTE abundance corrections turn out to be less than 0.1 dex for all the stars investigated. However, NLTE effects for the Ba II and Eu II lines are of opposite sign, and they are therefore important for a comparison of barium and europium abundances deduced from these lines.

3.3. Line profile calculations

Two Eu II lines relatively free of blends are used in Eu abundance estimations. Their atomic data are given in Table 3.

Radiative damping constants are computed explicitly: $\gamma_R = \sum_{i<u} A_{ui}$. Van der Waals damping constants C_6 are evaluated from the classical Unsöld (1955) formula, and the quadratic Stark effect is roughly estimated from the formula $\gamma_4 = N_e 10^{-8} n_{eff}^5$ where n_{eff} is the effective quantum number. Both Eu II lines are relatively weak ($W_\lambda < 60$ mÅ) in the stars investigated and only $\lambda 4129$ is slightly affected by collisional damping.

Eu II lines are strongly affected by hyperfine structure and isotopic shifts. Europium is represented by two odd isotopes with nearly equal contributions: for solar system matter their ratio ^{151}Eu: ^{153}Eu = 47.8: 52.2 according to Cameron (1982). Each isotope has hyperfine splitting of their levels. Laboratory data on HFS of the Eu II levels and isotopic shifts have been published by Krebs & Winkler (1960). The recent high resolution laser measurements of Broström et al. (1995) and Becker et al. (1993) for the Eu II resonance transition give results coinciding within error bars with the earlier data. The hyperfine splittings in the lower states, $6s\,^9\mathrm{S}^\circ$ and $5d\,^9\mathrm{D}^\circ$, are considerable larger than in upper ones. Then, transitions between a lower hyperfine level with total angular momentum F and upper levels with F-1, F, F+1 give three HFS components at rather

Table 3. Atomic data for the Ba II and Eu II lines. Most of the entries are self-explanatory; f_{ij} of the HFS components correspond to isotopic abundances of solar system matter for Ba and ^{151}Eu: ^{153}Eu = 55: 45 for Eu; in the column "isotope" we give the mass numbers of the isotopes responsible for the component; the collisional damping constants $\log C_6$ from solar line profile fitting are indicated

λ [Å] transition	HFS $\Delta\lambda$ [mÅ]	HFS f_{ij}	HFS isotope	$\log C_6$
Ba II 4554.03	0	0.597	138, 136, 134	–31.65
$6s\,^2\mathrm{S}_{1/2}$ - $6p\,^2\mathrm{P}^\circ_{3/2}$	18	0.081	137, 135	
	–34	0.049	137, 135	
Ba II 5853.70	–	0.025		–30.60
$5d\,^2\mathrm{D}_{3/2}$ - $6p\,^2\mathrm{P}^\circ_{3/2}$				
Ba II 6496.90	0	0.086	138, 136, 134	–31.30
$5d\,^2\mathrm{D}_{3/2}$ - $6p\,^2\mathrm{P}^\circ_{1/2}$	–4	0.012	137, 135	
	9	0.007	137, 135	
Eu II 4129.70	–97	0.007	151	–32.082
$6s\,^9\mathrm{S}^\circ_4$ - $6p\,^9\mathrm{P}_4$	–78	0.010	151	
	–52	0.013	151	
	–17	0.022	151, 153	
	–9	0.008	153	
	0	0.011	153	
	14	0.014	153	
	24	0.020	151	
	34	0.016	153	
	58	0.019	153	
	74	0.024	151	
Eu II 6645.10	–41	0.029	151, 153	–32.495
$5d\,^9\mathrm{D}^\circ_6$ - $6p\,^9\mathrm{P}_5$	–29	0.014	153	
	–18	0.023	151, 153	
	–10	0.011	153	
	–3	0.008	153	
	3	0.015	151, 153	
	11	0.001	151	
	23	0.009	151	
	38	0.007	151	
	50	0.005	151	

closely spaced wavelengths ($\Delta\lambda < 2$mÅ) and with intensities differing by much more than 10 times. In the present investigation the intensities of these three components are added. So, for each isotope the HFS is considered to consist of 6 main components which represent transitions from 6 hyperfine levels in the lower states. The intensity ratio between the main components is directly proportional to (2F + 1) of lower levels, and the oscillator strength of each component is calculated according to its relative intensity and isotopic abundance. We show in the next section that the solar Eu II λ4129 line profile is best fitted with an isotopic ratio ^{151}Eu: ^{153}Eu = 55: 45, and this ratio was used to obtain f_{ij} of the Eu II line components. Taking into account isotopic shift and superposition of some components both Eu II isotopes give 11 HFS components for the resonance line separated by 171 mÅ at maximum, and 10 HFS components for the subordinate line with 91 mÅ wide patterns (Table 3). Finally, we have adopted the component shifts obtained by Broström et al. (1995) for Eu II λ4129 and the values given by Biehl (1976) on the base of Krebs & Winkler (1960) data for Eu II λ6645.

The synthetic line profiles are computed using the departure coefficients b_i of the Eu II levels from the code NONLTE3 and the LTE assumption for other atoms. The line list is extracted from Kurucz' (1994) compilation, and it includes all the atomic and molecular lines.

4. Solar Ba II and Eu II lines

The Sun is chosen as reference star with an observed spectrum of high quality and relatively well-known stellar parameters. These data are used to improve two kinds of atomic data important for subsequent analyses of the metal-poor stars. These are the efficiency of hydrogen collisions in the Ba II and Eu II statistical equilibrium and van der Waals damping constants, C_6.

We use solar flux observations taken from the Kitt Peak Solar Atlas (Kurucz et al. 1984) and disk center intensity observations taken from the Preliminary Kitt Peak Solar Atlas (Brault & Testerman 1972). Our synthetic flux profiles are convolved with a profile that combines rotational broadening of 1.8 km s^{-1}and broadening by macroturbulence with a radial-tangential profile of $V_{\rm mac} = 2.6$ km s^{-1}for the Ba II lines and of larger values for the weaker Eu II lines: $V_{\rm mac} = 3.6$ km s^{-1}for λ4129 and $V_{\rm mac} = 3.8$ km s^{-1}for λ6645. The synthetic intensity profiles of the Eu II lines are convolved with a macroturbulence profile with $V_{\rm mac} = 2.4$ km s^{-1}.

4.1. Solar Ba abundance

In Paper I we showed that NLTE profiles give a better reproduction of the observations than LTE ones. However, with the NLTE method adopted for the Ba II lines and solar Ba abundance $\log \varepsilon_{\rm Ba,\odot} = 2.13$ from Anders & Grevesse (1989) we could not fit the line cores; the observed profiles of the Ba II subordinate lines λ5853 and λ6496 remained deeper by 3% of the continuum flux compared with the theoretical ones. In this study we reinvestigate solar Ba II lines. We use the NLTE method and the atomic model described in Paper I except for electronic collision cross-sections between the low excited Ba II terms 6s, 5d and 6p, for which we adopt the recent data by Schöning & Butler (1998). For the important forbidden transition 6s - 5d they result in about 10 times smaller values of the collision rates compared with the Crandall et al. (1974) data used in Paper I. In this case collisional coupling of the metastable level 5d to the ground state is weakened and NLTE effects are strengthened producing increased NLTE line depths of the λ5853 and λ6496 lines formed in the 5d - 6p transition. This makes it possible to fit solar Ba II line profiles (Fig. 3). In this study we neglect inelastic hydrogen collisions in statistical equilibrium of Ba II based on our subsequent analyses of metal-poor stars (Sect. 5.1). As it was discussed in Paper I solar Ba II lines are nearly insensitive to this factor.

Atomic data of the Ba II lines are given in Table 3. They are the same as in Paper I except for collisional damping constants C_6 that have been revised. As discussed in Paper I the 3-component model represents quite well the HFS components of the Ba II λ4554 line. Oscillator strengths of these components correspond to Ba isotope abundances of solar system matter from Cameron (1982), where (^{134}Ba+^{136}Ba+^{138}Ba): (^{135}Ba+^{137}Ba) = 82: 18. A depth-independent microturbulence of 0.8 km s^{-1}is derived from λ4554 and λ6496, and 0.75 km s^{-1}from λ5853. A *solar Ba abundance* $\log \varepsilon_{\rm Ba} = 2.21$ is obtained in this study, and this coincides with the meteoritic Ba abundance $\log \varepsilon_{\rm Ba} = 2.22 \pm 0.02$ from Grevesse et al. (1996). We emphasize that with $\log \varepsilon_{\rm Ba} = 2.13$, cited by Grevesse et al. 1996) as solar *photospheric* Ba abundance, the solar Ba II line profiles can not be reproduced.

It can be seen from Fig. 3 that fits to the subordinate lines are quite good, whereas for the resonance line the synthesized NLTE line core is still deeper than observed by about 2% of the continuum flux. To match the halfwidth of this line we are forced to increase $V_{\rm mac}$ to 3 km s^{-1}compared with the 2.6 km s^{-1}required to adjust the subordinate lines. As we discussed in Paper I the Ba II resonance line is formed in the uppermost atmospheric layers for normal metallicity F - G dwarfs, and it is most probably influenced by a non-thermal and depth-dependent chromospheric velocity field that is not part of our solar model (the chromospheric temperature rise is expected to be less important because Ba II is the dominant ionization stage). So, for the stars mentioned, it would be better to exclude the Ba II λ4554 from Ba abundance determinations.

4.2. Solar ^{151}Eu : ^{153}Eu ratio and europium abundance

Only two Eu II lines are relatively free of blending effects. The resonance line λ4129.7 is located in the far wing of the hydrogen line H_δ. In the solar spectrum H_δ contributes about 1% to the intensity at $\lambda = 4129.7$ Å. More important blending effects are due to the molecular line CN λ4129.595 and atomic lines Ti I λ4129.660 and Sc I λ4129.750 (Fig. 4). Their f_{ij} were corrected to improve the fit to the solar λ4129.7 *intensity* profile. However, we note that this procedure does not affect the final conclusions concerning Eu isotopic ratio and solar Eu abundance. The red line wing of the subordinate line Eu II λ6645.1 is blended by the

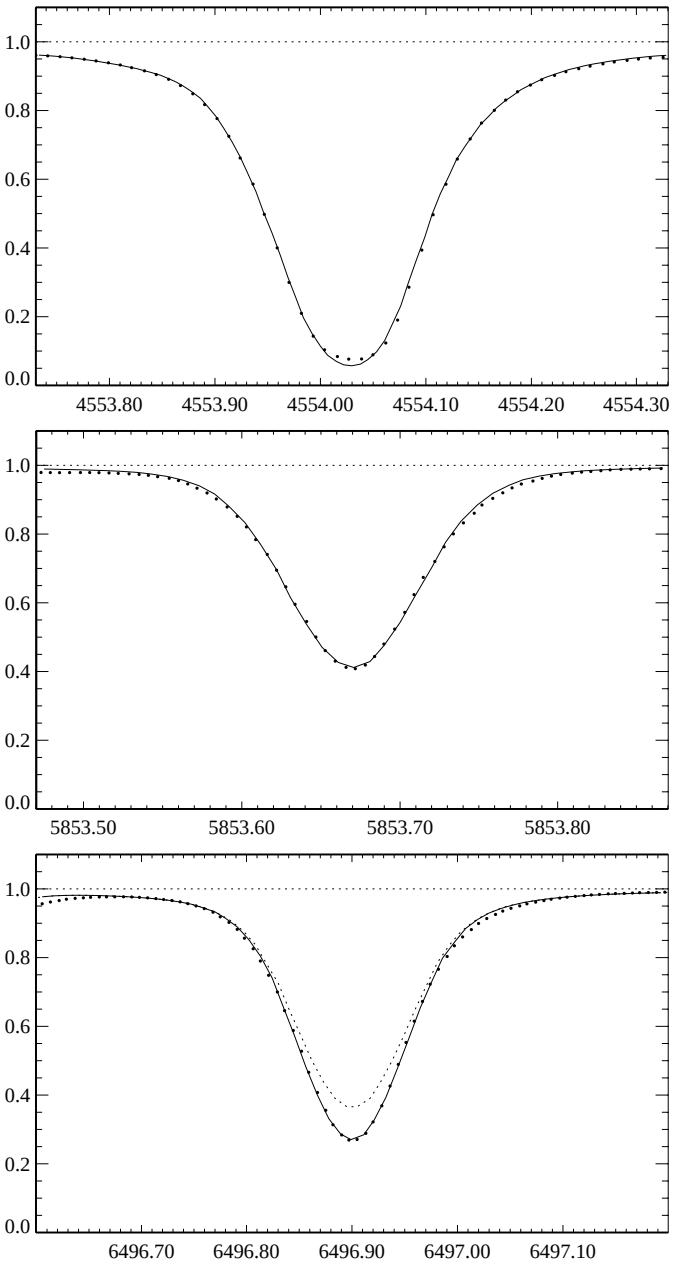

Fig. 3. Synthetic NLTE (continuous line) flux profiles of the Ba II lines compared with the observed spectrum of the Kurucz et al. (1984) solar flux atlas (bold dots). For the Ba II λ6496 the LTE profile (dotted line) is given too for comparison. See text for discussion of the fitting parameters

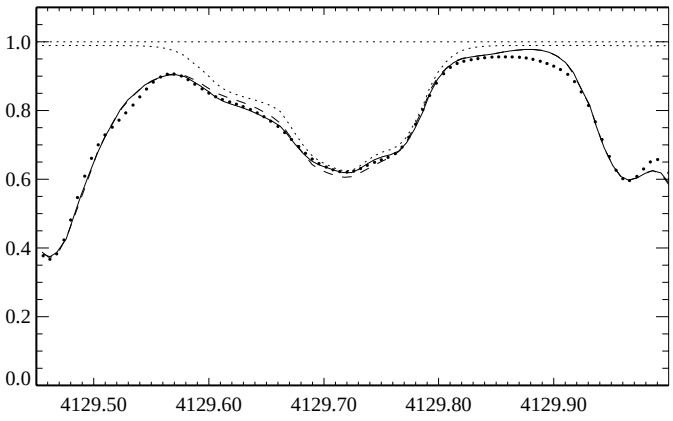

Fig. 4. Synthetic NLTE disk center intensity profiles of the Eu II λ4129 line for the isotopic ratios ^{151}Eu: ^{153}Eu = 55: 45 (continuous line) and 48.2: 51.8 (dashed line) compared with the observed spectrum of the solar disk center intensity atlas (Brault & Testerman 1972, bold dots). The pure Eu II line corresponding to Eu isotope ratio of 55: 45 is shown by dotted line. See text for discussion of the fitting parameters

Si I λ6645.20 Å line (Fig. 5). Atomic data of the Si I line have been taken from the Vienna Atomic Line Data Base (Kupka et al. 1999).

Both Eu II lines are nearly insensitive to variations of the microturbulence value. The subordinate line lies on the linear part of the curve of growth and the resonance line consists of 11 components with wavelength separation comparable with a Doppler half-width and each component is too weak to be sensitive to microturbulence. $V_{\rm mic} = 0.9$ km s^{-1}was adopted in calculating both intensity and flux line profiles.

As discussed in Sect. 3.3 the profile of the Eu II λ4129 is strongly asymmetric due to HFS and isotopic shifts. We note that the blue line wing is formed by the ^{151}Eu components, but the line core contains mainly the components of the second isotope (Table 3). The idea of improving Eu isotopic ratio was conceived after unsuccessful attempts to fit the solar Eu II λ4129 line with the terrestial ratio ^{151}Eu: ^{153}Eu = 47.8: 52.2 given by Cameron (1982). Intensity line profiles keep more details of the intrinsic profile since they are less affected by external broadening factors. That is why solar disk center intensity observations (Brault & Testerman 1972) were used to estimate the ^{151}Eu: ^{153}Eu ratio.

NLTE intensity profiles of the Eu II λ4129 line have been calculated for 4 isotope mixtures, where ^{151}Eu: ^{153}Eu = 47.8: 52.2, 50: 50, 52: 48 and 55: 45, respectively. In Fig. 4 we present the best fit corresponding to the ratio 55: 45 in comparison with the theoretical profile calculated at the terrestial isotope mixture. The subordinate line λ6645 profile is nearly insensitive to varying the Eu isotopic ratio because its blue wing and core are formed by the components of both isotopes. Using ^{151}Eu: ^{153}Eu = 55: 45 we can get a good fit of the solar Eu II λ4129 flux profile, too (Fig. 5), and the same Eu abundance $\log \varepsilon_{\rm Eu} = 0.53$ is derived from both intensity and flux profiles of this line.

An attempt to improve the solar Eu isotopic ratio was made by Hauge (1972). From fitting 6 solar Eu II line profiles he obtained ratios ^{151}Eu: ^{153}Eu ranging from 33: 67 to 64: 36, and thus deduced an average value of 52: 48. Strong blending effects for most of the Eu II lines used in his study were the reason for the large scatter of his results.

A *solar Eu abundance* $\log \varepsilon_{\rm Eu} = 0.53$ is obtained from both Eu II lines (Fig. 5). Our results are based on the laboratory oscillator strengths of Komarovskii (1991), $\log gf = 0.174$ for λ4129 and $\log gf = 0.204$ for λ6645 and NLTE analyses. With the LTE assumption we find $\log \varepsilon_{\rm Eu} = 0.49$ and 0.50 for the first and second line, respectively. NLTE effects weaken the

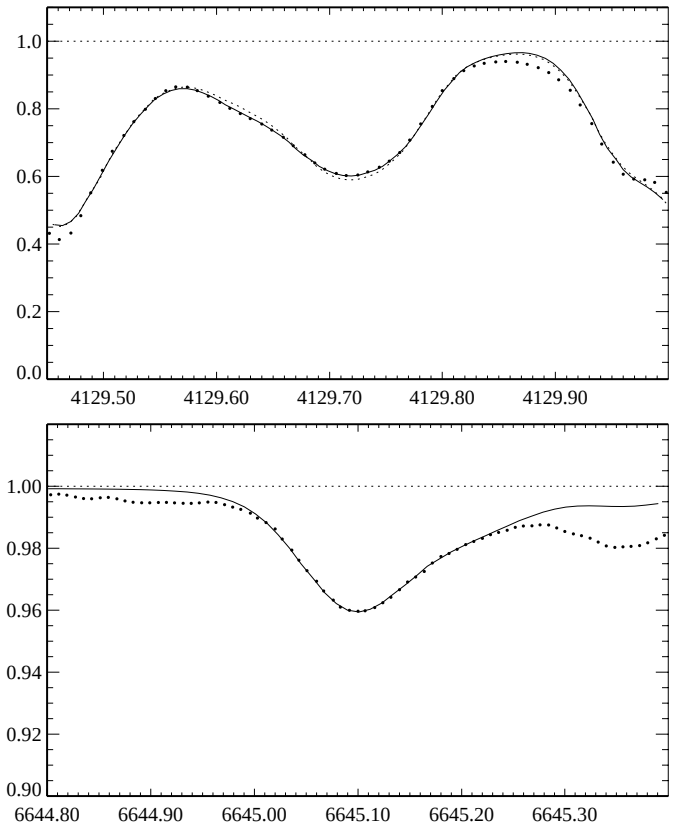

Fig. 5. Synthetic NLTE flux profiles of the Eu II lines compared with the observed spectrum of the Kurucz (1984) solar flux atlas (bold dots). In the top panel $\lambda 4129.7$ Å line profiles are presented for 2 isotopic ratios, ^{151}Eu: ^{153}Eu = 55: 45 (continuous line) and 48.2: 51.8 (dotted line). In the bottom panel the Eu II $\lambda 6645.1$ Å line profile (continuous line) is shown for ^{151}Eu: ^{153}Eu = 55: 45. See text for discussion of the fitting parameters

resonance line independent of the adopted efficiency of hydrogen collisions in the Eu II statistical equilibrium, and the NLTE abundance correction is positive. But $\lambda 6645$ arising from the metastable level is very sensitive to varying collision rates. Thus, it is strengthened compared with the LTE case if hydrogen collisions are neglected, and it is weakened if they are taken into account. We have found that hydrogen collision rates computed with the formula of Steenbock & Holweger (1984) should be multiplied by the factor $k_{\rm H}$= 1/3 to produce the best fit to the solar Eu II line profiles.

Grevesse et al. (1996) give $\log \varepsilon_{\rm Eu} = 0.55 \pm 0.02$ for the meteoritic Eu abundance and $\log \varepsilon_{\rm Eu} = 0.51$ for solar Eu abundance. We remember (Sect. 3.1) that with the atomic data available we underestimate the Eu II partition function and therefore also underestimate the solar Eu abundance by about 0.02–0.03 dex. Thus, our result coincides within the error bars with the meteoritic Eu abundance.

5. Results

Ba and Eu abundances are determined from line profile fitting of the stellar spectra. Only slow rotators were included in our sample, and therefore the instrumental profile acts as the dominant contributor to the convolution profile. The rotational velocity $V \sin i$ and macroturbulence value $V_{\rm mac}$ can not be separated at the spectral resolving power we have, and we treat their total action as radial-tangential macroturbulence. With the known instrumental profile $V_{\rm mac}$ is deduced from the observed line shape. The spectra observed at $R = 60000$ are well fitted and for each star the values of $V_{\rm mac}$ from different Ba II and Eu II lines coincide within 0.4 km s^{-1}. Elemental abundances are derived from these spectra with an uncertainty not larger than 0.02 dex. At $R = 40000$ the observed profiles are well fitted for stars with [Fe/H] > -0.6, but at lower metallicities the Ba II $\lambda 5853$, $\lambda 6496$ and Eu II $\lambda 4129$ are badly fitted in a few cases, and we estimate the uncertainty of their abundances by 0.05–0.10 dex. The less reliable results are marked by ":" in Table 1. As an example, we give in Fig. 6 and 7 both the Ba II and Eu II line profiles for stars of different metallicity.

5.1. Barium abundances for the stars

Barium abundances have been determined for the 29 stars listed in Table 1; for 23 of them abundances are obtained for all three Ba II lines. The weakest Ba II line $\lambda 5853$ disappears at [Fe/H] < -1.9. In addition, $\lambda 6496$ was not used in the analyses of HD 19445 and BD $34°2476$ because of its superposition with telluric lines. For BD $29°366$ only the blue spectral range was observed. Consequently, for the three stars mentioned, Ba abundances have been derived only from the Ba II resonance line $\lambda 4554$.

HFS affecting the Ba II lines was discussed in detail in Paper I. Only for the resonance line $\lambda 4554$ this effect is important. We follow Paper I and accept in this study the 3-component model to describe HFS components of Ba II $\lambda 4554$. Their oscillator strengths (Table 3) correspond to a solar ratio of the even-to-odd Ba isotopes, 82: 18 (Cameron 1982). We show below (Sect. 5.3) that barium seen in the halo and thick disk stars must have been mainly produced by the r-process. It means we should use for these stars the pure r-process isotopic ratio. However, an uncertainty of the r-process contribution to the important even isotope ^{138}Ba (^{134}Ba and ^{136}Ba are synthesized only by the s-process) is rather large. According to recent estimations of Arlandini et al. (1999) it is about 59%. During the last twenty years the pure r-process ratio ^{138}Ba: (^{135}Ba + ^{137}Ba) varied from 28: 72 (Cameron 1982) to 56: 44 (Arlandini et al. 1999). In Sect. 5.4 we will show that the change in Ba abundance with varying even-to-odd isotopic ratio over the acceptable range of values is below 0.05 dex for HD 19445 and BD $34°2476$ and 0.1 dex for BD $29°366$.

NLTE effects for Ba II in cool stars were described in detail in Paper I. Here we just remember that the statistical equilibrium of Ba II is strongly affected by radiative processes in b-b transitions because this is the dominant ionization stage. As a consequence NLTE effects for Ba II depend on the Ba abundance which correlates with the general metallicity of the model atmosphere. Thus, NLTE leads to a strengthening of the Ba II lines compared with the LTE case at [M/H] > -1.9 and to the

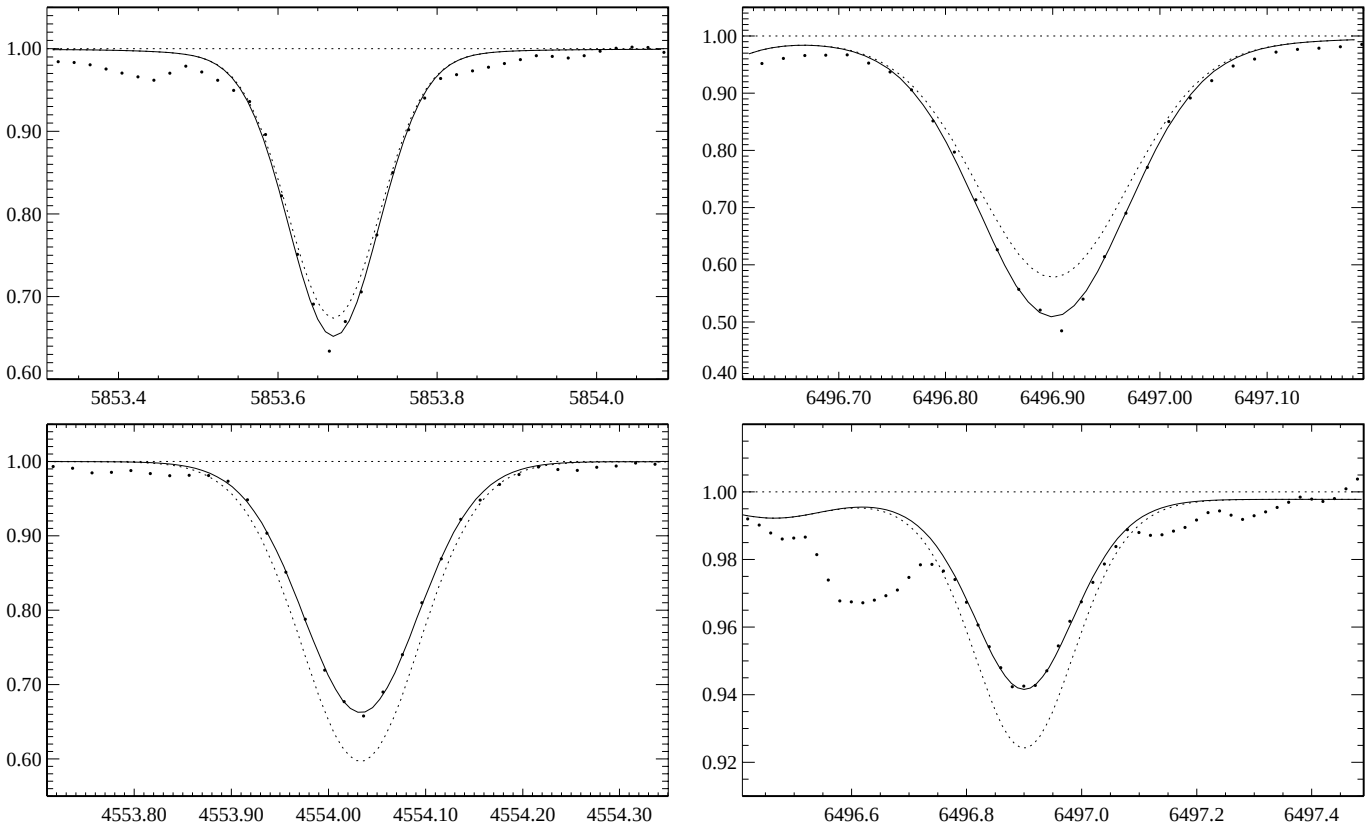

Fig. 6. Synthetic NLTE (continuous line) and LTE (dotted line) flux profiles of Ba II lines compared with the observed FOCES spectra (bold dots) of HD 157214 ([Fe/H] $= -0.34$, up row) and HD 84937 ([Fe/H]$= -2.07$, low row). $\lambda/\Delta\lambda = 60000$. For HD 157214 the ratio [Ba/Fe] of -0.13 is estimated from $\lambda5853$ and of -0.13 from $\lambda6496$. For HD 84937 the corresponding values of -0.01 and $+0.01$ are obtained from $\lambda4554$ and $\lambda6496$.

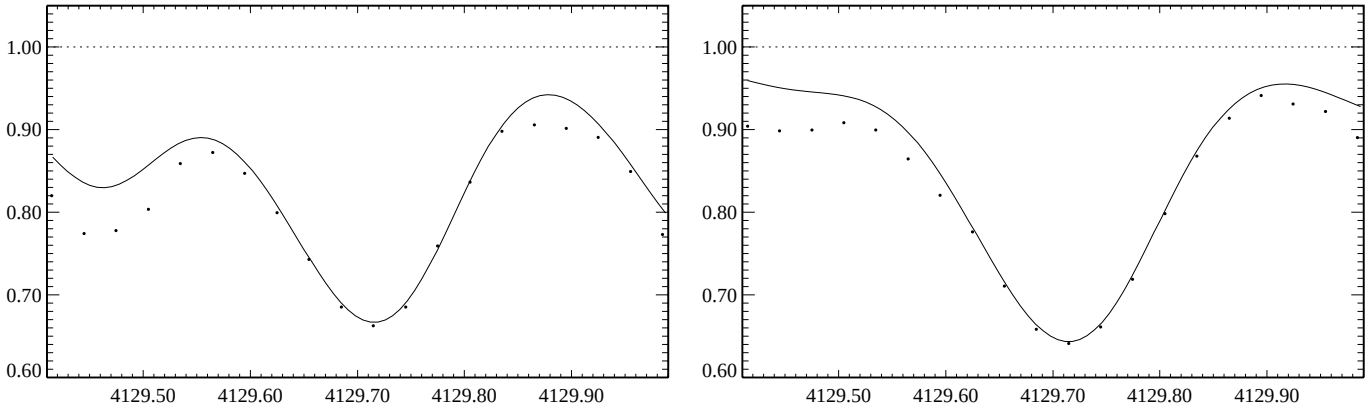

Fig. 7. Synthetic NLTE (continuous line) flux profiles of Eu II lines compared with the observed FOCES spectra (bold dots) of HD 184499 ([Fe/H] = -0.51, left panel) and HD 45282 ([Fe/H] = -1.52, right panel). $\lambda/\Delta\lambda = 40000$. Continuum level is fixed by fitting observed spectra in the spectral range from 4123 Åto 4135 Å.

opposite effect at lower metallicities. NLTE effects are small for the weakest line $\lambda5853$ and at [M/H] > -1.9 for the resonance line $\lambda4554$. In terms of NLTE abundance corrections $\Delta_{\rm NLTE} = \log\varepsilon_{\rm NLTE} - \log\varepsilon_{\rm LTE}$ they do not exceed 0.1 dex by absolute value. For the most metal-poor stars $\Delta_{\rm NLTE}$ becomes positive and reaches 0.22 dex for $\lambda4554$ in HD 84937 ([Fe/H] = -2.07). Significant NLTE effects have been found for the second subordinate line $\lambda6496$. $\Delta_{\rm NLTE}$ is –0.2 dex on average in the metallicity range $-1 <$[Fe/H]< 0.1; it is reduced by absolute value to 0.10–0.15 dex at metallicities between –1.5 and –1, and it becomes positive up to 0.15 dex at even lower [Fe/H]. If NLTE effects are neglected Ba abundances from $\lambda4554$ and $\lambda6496$ show a false decline from about [Ba/Fe] = 0.1 at normal metallicity to -0.2 at [Fe/H] = -2.1.

In Fig. 8 we compare Ba abundances calculated from two subordinate lines revealing rather different NLTE effects. To re-

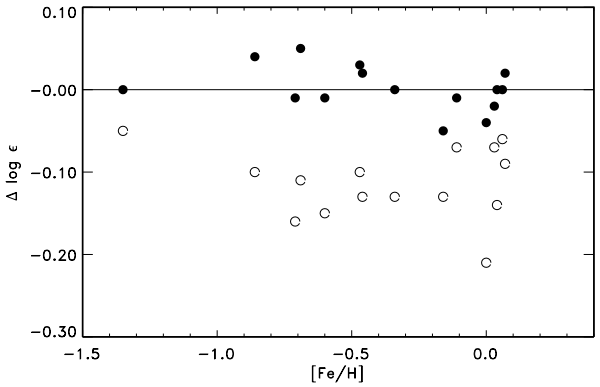

Fig. 8. Comparison of barium abundances derived from the Ba II $\lambda5853$ and $\lambda6496$ lines. Symbols correspond to NLTE (filled circles) and LTE (open circles) abundance differences $\Delta \log \varepsilon = \log \varepsilon(\lambda5853) - \log \varepsilon(\lambda6496)$

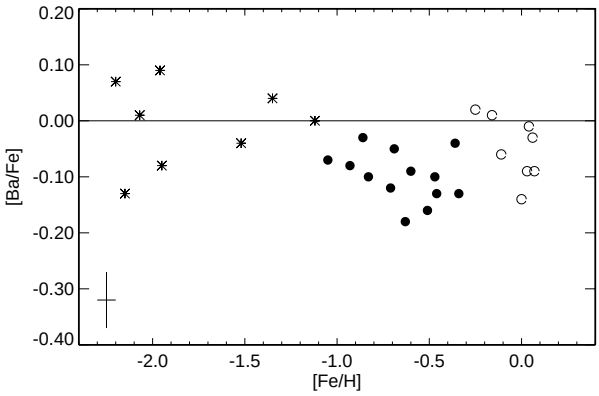

Fig. 9. The run of [Ba/Fe] with [Fe/H]. Symbols correspond to the thin disk (open circles), the thick disk (filled circles) and the halo (asterics) stars. Error bars are indicated

duce observational errors only the results based on the best quality spectra ($R = 60000$) are presented. It can be seen that there are no systematic discrepancies between NLTE abundances derived from $\lambda5853$ and $\lambda6496$, and the scatter of the difference between them does not exceed $\pm$ 0.05 dex. This gives reason to believe that the uncertainty of our NLTE line formation treatment leads to Ba abundance errors not greater than 0.05 dex. Fig. 8 shows clearly that the LTE abundances from $\lambda6496$ are systematically overestimated relative to $\log \varepsilon_{\rm LTE}(\lambda5853)$.

Thus, for 26 stars we have obtained Ba abundances from the subordinate lines. If both of them were available the average value was calculated. For the three stars mentioned, with only the resonance line available, Ba abundances have been obtained from this line at the assumption of a solar even-to-odd Ba isotope ratio. It is evident from Fig. 9 that taking into consideration the data for these three stars does not change the conclusions. The final [Ba/Fe] are presented in Table 1. As the reference solar abundances $\log \varepsilon_{\rm Ba,\odot} = 2.21$ deduced from fitting solar Ba II line profiles (Sect. 4.1) and $\log \varepsilon_{\rm Fe,\odot} = 7.51$ adopted by Fuhrmann (1998, 2000) in stellar metallicity determinations are used.

Fig. 9 shows the plot of [Ba/Fe] versus metallicity, strongly suggestive of membership in a particular population of the Galaxy. We find that Ba is slightly underabundant by about 0.1 dex relative to iron in the thick disk stars. For the halo stars the abundance ratios [Ba/Fe] are nearly solar. The scatter of data is up to 0.2 dex.

The common conclusion of most recent researches of barium abundances (Gratton & Sneden 1994; Woolf et al. 1995; Jehin et al. 1999; Chen et al. 2000) is that the barium abundance follows iron at [Fe/H] > -2, independent of metallicity. The largest samples of stars in a metallicity range similar to ours were considered by Woolf et al. (1995) and Chen et al. (2000). A rather large scatter of data up to 0.5 dex for stars of similar metallicities is typical for the work of Woolf et al., and this might have masked a slight Ba underabundance in mildly metal-deficient stars found in our study. It is interesting that Chen et al. (2000) find even an overabundance of Ba relative to iron of about 0.1 dex in the metallicity range $-0.8 <$ [Fe/H] < -0.2. Their results are based on three Ba II subordinate lines $\lambda5853$, $\lambda6141$ and $\lambda6496$. We have shown above that NLTE effects for the $\lambda6496$ line are significant and lead to an overestimate of Ba abundances up to 0.25 dex. We do not use the Ba II $\lambda6141$ line because of its blending with an Fe I line, but our NLTE calculations show that NLTE effects for this line are not smaller than for $\lambda6496$. So, we expect that neglecting NLTE effects for Ba II lines has resulted in too high Ba abundances in the work of Chen et al. (2000).

5.2. Europium abundances for the stars

Europium abundances have been calculated for 15 stars of our sample. Only the spectra observed at $R = 40000$ were used in the Eu II $\lambda4129$ line analyses. The higher resolution spectra will be reduced and investigated in future work. For the stars with [Fe/H] ≤ -1.9 the Eu II line can not be extracted from noise and only the upper limit of Eu abundance could be estimated for HD 19445, BD 66°268 and BD 34°2476, [Eu/Fe] ≤ 0.5. In total, for 11 stars Eu abundances have been obtained from the Eu II resonance line. The subordinate line $\lambda6645$ is too weak, and it was analyzed only for one star, HD 187691, which has the largest metallicity, [Fe/H] = 0.07. For this star NLTE europium abundances from $\lambda4129$ and $\lambda6645$ are found to coincide within 0.01 dex. The $\lambda6645$ line has also been detected and analyzed for 4 mildly metal-poor stars with spectra observed at $R = 60000$ in January 1999 (HD 30649, HD 69611 and HD 102158) and in May 1997 (HD 157214). Those observing runs are distinguished by good atmospheric conditions and a narrow instrumental profile. The Eu II $\lambda6645$ line is blended by the Si I line and we have supposed that silicon abundance in these stars follows magnesium abundance.

As discussed in Sect. 3 NLTE effects weaken both Eu II lines compared with the LTE case and NLTE abundance corrections are positive. For the stars of our sample $\Delta_{\rm NLTE}$ ranges from 0.04 dex up to 0.08 dex for the resonance line and from 0.04 dex up to 0.06 dex for the subordinate line.

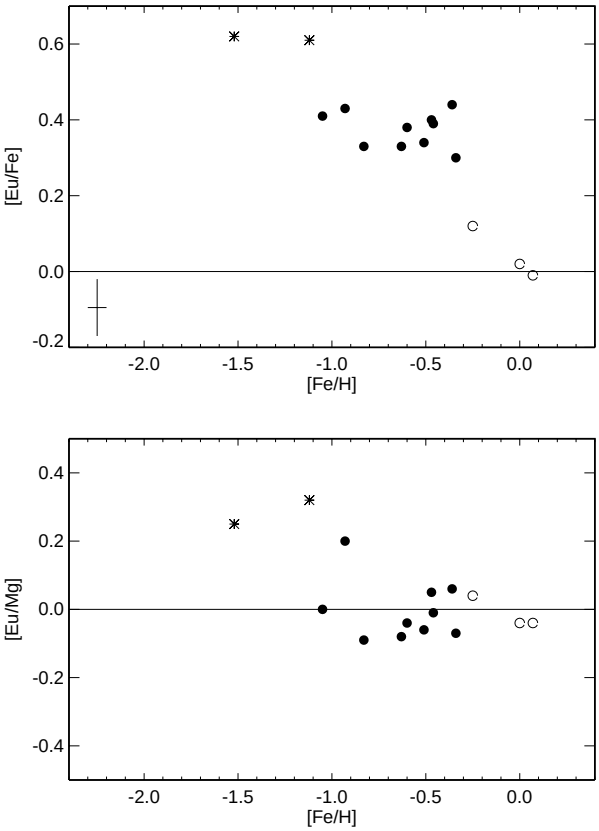

Fig. 10. Variation of [Eu/Fe] (top panel) and [Eu/Mg] (bottom panel) with [Fe/H]. Symbols are the same as in Fig. 9

NLTE europium abundances relative to iron are presented in Table 1 and in Fig. 10 (top panel). As the reference solar Eu abundance $\log \varepsilon_{\mathrm{Eu},\odot} = 0.53$ deduced from fitting solar Eu II line profiles (Sect. 4.2) is adopted. It can be seen that the halo and thick disk stars reveal a strong Eu overabundance relative to iron. In thick disk stars the [Eu/Fe] ratios range from 0.30 to 0.44 and there is a hint of slight decline of this ratio with metallicity increasing. The higher values of [Eu/Fe] = 0.61 and 0.62 have been obtained for two halo stars.

An overabundance of europium relative to iron in metal-poor stars was found in earlier work (Woolf et al. 1995, and references therein). Most Eu abundances previously available for stars in the metallicity range covered in this study are from the work of Woolf et al. (1995) and Jehin et al. (1999), in which the data are reported for 81 field F and G disk dwarfs with [Fe/H] ≥ -0.9 and for 21 mildly metal-poor ($-1.2 \geq$ [Fe/H] ≤ -0.6) unevolved stars, respectively. In the first work a steady increase in the abundance ratio [Eu/Fe] from -0.1 to 0.4 is obtained with decreasing metallicity. However, Woolf et al. (1995) note that the [Eu/Fe] ratio depends on the Galactocentric radius R_m. If we look at Fig. 8 (top panel) of their paper where only the stars from the inner Galaxy ($R_m \leq 7$) kpc are given we find a nearly constant value of [Eu/Fe] $\simeq 0.23$ in the metallicity range [Fe/H] ≤ -0.4 and a discontinuity for [Eu/Fe] at [Fe/H] $\simeq -0.4$. This looks like the behaviour of [Eu/Fe] obtained in this study except for that we have found the larger values of [Eu/Fe] at metallicities below -0.4. From twelve Woolf et al. (1995) stars with $R_m \leq 7$ and [Eu/Fe] > 0.1 seven stars turn out to be thick disk stars according to Fuhrmann (1998, 2000). Thus the question is whether Fig. 8 from Woolf et al. (1995) reflects a difference between the inner and outer Galaxy or a difference between the thick and thin disk stellar populations of the Galaxy. Jehin et al. (1999) give even weaker europium overabundances relative to iron ranging mainly between 0 and 0.2. For the halo stars the results of different authors diverge significantly. Gratton & Sneden (1994) have found small ratios [Eu/Fe] of about 0.1–0.2, but Magain (1989) gives much larger values up to 0.7 in the same range of metallicities.

Thus, we have obtained enhanced europium-to-iron abundances in the halo and thick disk stars. The behaviour of the [Eu/Fe] ratios versus metallicity is very similar to overabundances found for the α-process elements, oxygen, magnesium and others (see McWilliam 1997, for a review). This should be expected because both the α- and r-process elements are commonly believed to be produced in SN II events. In Fig. 10 (bottom panel) we give the ratios of europium abundances estimated in present study to magnesium abundances in the same stars evaluated by Fuhrmann (1998, 2000). The europium abundances follow the magnesium abundances in the thick and thin disk stars and it was expected. For the two halo stars a weak Eu-to-Mg overabundance of about 0.2 dex is found and the larger number of halo stars should be investigated to make clear whether that overabundance is real.

5.3. Abundance ratios [Eu/Ba]

The abundance ratios [Eu/Ba] are shown in Fig. 11 versus metallicity indicating a membership to the particular population of the Galaxy. The new results found in this study are

1. europium is overabundant relative to barium in the halo and thick disk stars; thick disk stars form a plateau with [Eu/Ba] = 0.49 $\pm$ 0.03, and higher values of [Eu/Ba] = 0.61 and 0.66 have been obtained for two halo stars;
2. there is an abrupt change in [Eu/Ba] ratio as one goes from the thick to thin disk stars.

The europium-to-barium abundance ratio provides a useful diagnostic of the neutron capture processes that formed the heavy elements. This ratio for a pure r-process $\log$ (Eu/Ba)$_r$ equals -0.98 according to the most recent data of Arlandini et al. (1999) that translates to [Eu/Ba]$_r$ = 0.70 provided that the ratio between solar Eu and Ba abundances evaluated in this study $\log$ (Eu/Ba)$_\odot$ = 0.53–2.21 = -1.68 is adopted. A line indicating [Eu/Ba]$_r$ = 0.70 for a pure r-process is included in Fig. 11. The observed [Eu/Ba] ratios for two halo stars, close to 0.70 and the high mean value [Eu/Ba] = 0.49 found for the thick disk stars favour a dominance of the r-process in heavy element production at times of the halo and thick disk formation. The lower abundance ratios in the thick disk stars, compared with 0.70 values of [Eu/Ba], permit up to 30% of barium to have been produced by the s-process.

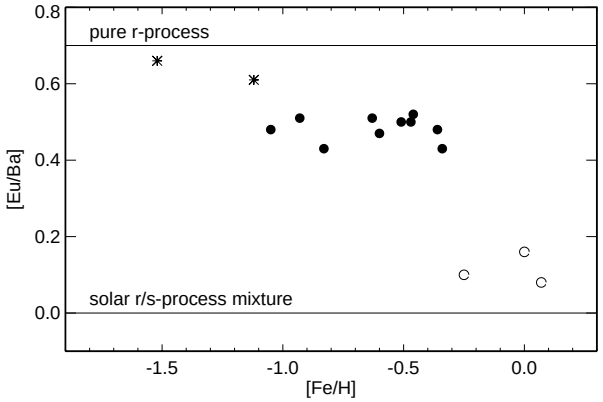

Fig. 11. Variation of [Eu/Bu] with [Fe/H]. Symbols are the same as in Fig. 9

We have only two halo stars and this limits us to draw reliable conclusions concerning a halo. Nevertheless, our results for two moderately metal-deficient halo stars ([Fe/H] = -1.12 and -1.50) turn out to agree well with the data of McWilliam (1998) who has obtained [Eu/Ba] ratios between 0.5 and 0.85 with the mean value of [Eu/Ba] = 0.69 for the sample of extremely metal-poor stars with [Fe/H] ≤ -2.4. We infer from this that the halo stellar population reveals the almost pure r-process heavy element composition independent of metallicity. From the insignificant contribution of the s-process to Ba production we conclude that the halo stellar population has formed quickly during an interval smaller than an evolution time of a 4 $M_\odot$ star, which is thought to be the upper mass limit of AGB stars' progenitors, responsible for Ba synthesis in the s-process (Travaglio et al. 1999). According to Massevich & Tutukov (1988) an evolution time of such stars is about 160 million years.

Our data show for the first time a high overabundance of Eu relative to Ba in the *thick disk* stars which means that the epoch of this stellar population formation was rather short because s-process element production, even if it was switched on, could not enrich interstellar matter with significant amounts of Ba. This observational finding constitutes a constraint to the duration of that epoch.

No significant overabundance of Eu relative to Ba is found in the three thin disk stars with Eu abundances available, and an exciting feature is the step-like decrease of the [Eu/Ba] ratio at the thick-to-thin disk transition. This result suggests there was a phase before the onset of the thin disk stellar population formation during which r-process element and iron production stopped but s-process nuclei of Ba were synthesized in evolved low mass stars. Thus, that phase was characterized by nearly ceased star formation and its duration is constrained by the time needed to increase the Ba abundance in the interstellar gas up to the values observed in the thin disk stars. We note such a hiatus in star formation was suggested by Fuhrmann (1998) on the base of magnesium and iron abundance analyses. The age-metallicity relation deduced by Ng & Bertelli (1998) is also indicative of a star formation gap on their stellar age scale between 10–12 Gyr.

Although no previous study of Eu and Ba abundances found such a step-like change of the [Eu/Ba] ratio we have inspected the data by Woolf et al. (1995) and find that they are suggestive of such a behaviour. Fig. 11 from their paper gives the [Eu/Ba] ratios versus [Fe/H] for different ranges of Galactocentric radius. It can be seen that the metal-poor stars ([Fe/H] ≤ -0.3) form a plateau with [Eu/Ba] = 0.4 if they are inside 7 kpc and with a [Eu/Ba] value smaller by about 0.2 dex if they are outside 7 kpc. A graduate decrease in the [Eu/Ba] ratio to -0.1 is seen at higher metallicities. From the perspective that two different stellar populations are involved in Fig. 11 of Woolf et al. (1995) (see Sect. 5.2) the behaviour of their [Eu/Ba] ratios is similar to that found in this study. However, their elemental abundances are based on the LTE assumption resulting in a lower value of [Eu/Ba] = 0.4 for the thick disk stars compared with our value of [Eu/Ba] = 0.49.

5.4. The r/s-process controversy from the Ba II *λ4554 line*

In Paper I we suggested a direct method of determining the odd-to-even isotopic ratio from the Ba II resonance line provided that the Ba total abundance is determined from the subordinate Ba II lines. The resonance line of the odd isotopes has several HFS components and this leads to an additional broadening of the line. HFS components of each odd isotope are disposed by two groups shifted relative to the resonance line of even isotopes by 18 mÅ and -34 mÅ, respectively. So, the 3-component simplification suggested by Rutten (1978) is sufficiently precise and the relative strengths of these components depend on the odd-to-even isotopic ratio. The larger the fraction of odd isotopes is, the broader is the spectral line and the greater is the total energy absorbed in the resonance line.

In Paper I we have shown for the metal-poor stars in the metallicity range $-2.20 \geq$ [Fe/H] ≤ -0.83 that, at Ba abundances derived from the Ba II subordinate lines free of HFS splitting, the even-to-odd isotopic ratios estimated from the resonance line are close to solar ratio 82: 18 (Cameron 1982). Based on the pure r-process even-to-odd isotopic ratio 28: 72 from Cameron (1982) and on the observed small fraction of the odd isotopes we inferred that there are no observational arguments for the hypothesis that the r-process dominated Ba production at early phases of the Galactic evolution. But the opposite conclusion is drawn in this study from analyses of the [Eu/Ba] ratios. Here we try to make this point clear.

We have derived barium abundances from the λ4554 line in the halo and thick disk stars for two even-to-odd Ba isotope mixtures, for a solar ratio 82: 18 and for a ratio 54: 46 corresponding to a pure r-process Ba production according to the most recent data of Arlandini et al. (1999). We name these abundances $\log \varepsilon_{4554}$(solar) and $\log \varepsilon_{4554}$(r). If at times of the halo and thick disk formation barium was mainly synthesized by the r-process $\log \varepsilon_{4554}$(r) should coincide within error bars with the barium abundance from the subordinate lines, $\log \varepsilon$(subord), and $\log \varepsilon_{4554}$(solar) would be overestimated. In Fig. 12 we compare the differences $\Delta \log \varepsilon_{\rm s} = \log \varepsilon_{4554}$(solar)$- \log \varepsilon$(subord) and $\Delta \log \varepsilon_{\rm r} = \log \varepsilon_{4554}$(r) $- \log \varepsilon$(subord). It can be seen that $\log \varepsilon_{4554}$(solar) is on average higher than $\log \varepsilon$(subord) in the halo and thick disk stars. But this is true for the thin

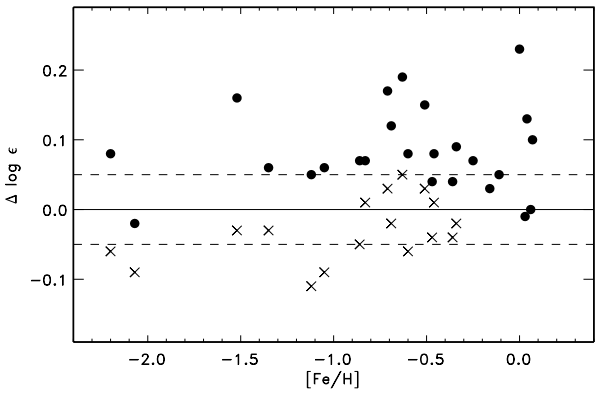

Fig. 12. Comparison of barium abundances derived from the Ba II $\lambda 4554$ and subordinate lines. Symbols correspond to $\Delta \log \varepsilon_{\rm s}$ = $\log \varepsilon_{4554}$(solar) – $\log \varepsilon$(subord) (filled circles) and $\Delta \log \varepsilon_{\rm r}$ = $\log \varepsilon_{4554}({\rm r}) - \log \varepsilon$(subord) (crosses). Dashed lines limit the range of possible abundance errors

disk stars, too, though no significant deviation of the Ba isotope mixture from the solar one is expected for these stars. In addition, we note that the hotter normal metallicity stars are, the larger is the difference $\Delta \log \varepsilon_{\rm s}$. For 3 thin disk stars with $T_{\rm eff} \geq 6000$ K $\Delta \log \varepsilon_{\rm s} \geq 0.1$. In Paper I we discussed divergences between Ba abundances obtained from the resonance and subordinate lines for the Sun and Procyon. The resonance line core of these stars is formed in the uppermost atmospheric layers near $\log \tau_{5000} = -4.5$, and it is most probably influenced by a non-thermal and depth-dependent chromospheric velocity field. Similar effects are expected for other stars with metallicities close to solar. With decreasing metallicity resonance line formation is shifted towards deeper layers and the chromospheric influence is reduced. However, it can still be important for mildly metal-deficient stars with [Fe/H] as low as -0.5. The large value of $\Delta \log \varepsilon_{\rm s} = 0.16$ for the metal-poor star HD 45282 ([Fe/H] $= -1.5$) may also reflect chromospheric influence because it is the most luminous star of our sample with the most extended atmosphere, and the $\lambda 4554$ line core is formed near $\log \tau_{5000} = -3.6$.

It can be seen from Fig. 12 that nearly for all our halo and thick disk stars the Ba abundance derived from the $\lambda 4554$ line assuming pure r-process barium production is closer to the abundance from the subordinate lines, and that $\Delta \log \varepsilon_{\rm r}$ is within error bars. The exception is two stars, HD 194598 and HD 201891, with an uncertainty of $\log \varepsilon$(subord) greater than $\pm$ 0.05 dex (see Table 1), and the halo star HD 84937 where $\log \varepsilon$(subord) was obtained from the only week line $\lambda 6496$ and the abundance error is expected also greater than $\pm$ 0.05 dex.

We emphasize that the possibility to differentiate between Ba abundances obtained from the $\lambda 4554$ line at the solar and pure r-process Ba isotope mixture is reduced as one changes from Cameron (1982) to Arlandini et al. (1999) data. For example, we showed in Paper I that the pure r-process $\lambda 4554$ line is deeper than the observed one in BD 66°268 and that, in order to agree with observations, the Ba abundance would have to be reduced by 0.2 dex. If that analysis would be performed with the data of Arlandini et al. (1999) the Ba abundance would have to be reduced by a smaller value of 0.13 dex which is, in fact, within the error bars because for this metal-poor star ([Fe/H] $= -2.20$) only the weak subordinate line $\lambda 6496$ is observed, and $\log \varepsilon$(subord) is derived with an uncertainty of about 0.1 dex. In this paper we have revised our Ba abundances on the base of the advanced NLTE method for Ba II. As a result, the difference between $\log \varepsilon_{4554}$(r) and $\log \varepsilon$(subord) in BD 66°268 has reduced to 0.06 dex, but $\Delta \log \varepsilon_{\rm s}$ has increased to 0.08 dex. Though the new results tend to reveal a significant contribution of the r-process to Ba production, the difference $\log \varepsilon_{4554}$(solar) $- \log \varepsilon_{4554}$(r) is not large enough to infer with confidence whether r- or s-process played a dominant role at the epoch of this star's formation. Even smaller values of $\log \varepsilon_{4554}$(solar) $- \log \varepsilon_{4554}$(r) = 0.06–0.09 are found for other halo stars, HD 103095, HD 84937.

Thus, with more confidence for thick disk than for halo stars our analyses of HFS affecting the Ba II resonance line using the new data of Arlandini et al. (1999) give arguments in favour of a higher fraction of the odd Ba isotopes compared with the solar one and, therefore, a dominance of r-process nucleosynthesis of heavy elements. However, a change in broadening the $\lambda 4554$ line between two extreme cases (a pure r-process and solar r/s-process mixture) is relatively small for stars with metallicities smaller than -1 and this reduces the use of our method based on the analysis of HFS affecting this line to estimate the r/s-process ratio in heavy element production.

6. Conclusions

Elemental abundance ratios [Ba/Fe] have been estimated for 29 stars in the range of metallicity $-2.20 \leq$ [Fe/H] ≤ 0.07 and the [Eu/Fe] and [Eu/Ba] ratios for 15 stars with [Fe/H] between -1.50 and 0.07. An important advantage of our study is provided by taking into account a membership of individual stars to particular stellar populations of the Galaxy. Such an approach was first suggested by Fuhrmann (1998) in his study of magnesium to iron abundance ratios, and it has been extended recently by Fuhrmann (2000) on the basis of a considerably enlarged sample.

We sum up the above results.

1. Europium is overabundant relative to iron in the halo and thick disk stars: 10 thick disk stars show [Eu/Fe] ratios between 0.30 and 0.44, and a slight decline of this ratio with metallicity can be seen; for two halo stars [Eu/Fe] = 0.62.
2. Barium abundances follow iron in the halo and thin disk stars though a scatter up to 0.2 dex occurs. In the thick disk stars barium is slightly underabundant by about 0.1 dex.
3. Europium is overabundant relative to barium in the halo and thick disk stars with the mean values [Eu/Ba] = 0.64 and 0.49, respectively.
4. There is an abrupt decrease in the [Eu/Ba] ratio at the transition from thick to thin disk stars.

These data give useful information for chemical evolution and for the evolution of stellar populations of the Galaxy.

From observed [Eu/Ba] ratios close to the pure r-process value of $[\mathrm{Eu/Ba}]_\mathrm{r} = 0.70$ (Arlandini et al. 1999) and analyses of HFS affecting the Ba II resonance line it follows that *heavy elements in the halo and thick disk stars were produced mainly in an r-process environment*. Truran (1981) was one of the first who suggested that the r-process dominated the production of heavy elements in very metal-poor stars. Some abundance studies of halo stars gave arguments for this hypothesis. Sneden & Parthasarathy (1983), Gilroy et al. (1988) and Sneden et al. (1996) found the heavy element abundance patterns consistent with nucleosynthesis dominated by the r-process. McWilliam (1998) has obtained [Eu/Ba] ratios close to pure r-process for a sample of extremely metal-deficient stars with $[\mathrm{Fe/H}] \leq -2.4$. Our analysis shows clearly that this is not a matter of a star's metallicity, but the age of a star or the membership in Galactic stellar populations is important. Insignificant s-process contributions to barium observed in the thick disk stars constrain *the duration of formation of this stellar population by the time comparable with the evolution time of intermediate mass AGB progenitors*. Thus, the thick disk must have formed quickly from the point of view of the Galaxy time scale and *the thick disk stars are old stars formed at the epoch when the interstellar gas was mainly enriched by SNII events*. We find support to this statement in Fig. 11 of Fuhrmann (1998) where stellar ages are indicated. It can be seen from that figure that the most of thick disk stars may be as old as $\sim$ 12–14 Gyr. The two halo stars with the calculated ratios [Eu/Ba] do not allow us to study with a confidence a history of the halo. Extended Eu abundance determinations will be presented in a separate study.

Abrupt changes in [Eu/Ba] ratio at the thick-to-thin disk transition indicate clearly *an intermediate phase characterized by ceased star formation*. Europium and barium enrichment from SNII events had come to an end but barium started to be produced by the s-process in evolved low mass stars. The duration of this phase is defined by the time needed to increase the Ba abundance in the interstellar gas up to the values observed in thin disk stars. The onset of the Galactic thin disk formation is referred to by some authors (Fuhrmann 1998, 2000; Edvardsson et al. 1993; Ng & Bertelli 1998) to the epoch 9–10 Gyr ago.

Acknowledgements. ML acknowledges with gratitude the Max-Planck-Institut of Astrophysics for the partial support of this study and the Institute of Astronomy and Astrophysics of Munich University for warm hospitality during a productive stay in September - December 1999. The authors thank Klaus Fuhrmann for providing the reducted FOCES spectra of the most of stars investigated in this paper and the parameters of 11 stars before publication, for valuable help and many useful discussions. The authors are grateful to Johannes Reetz for providing the code SIU for synthetic spectrum computations, Frank Grupp and Andreas Korn for providing the reduced FOCES spectra for some of the stars and the stellar parameters for BD 29°366 and BD 34°2476, Keith Butler for the discussion of the Eu II partition function, and Klaus Wisshak for the discussion of the r-process contribution to ^{138}Ba. ML has been partially supported by the Russian Basic Researches Fund (grant 99-02-17488).

References

Allen C.W., 1973, Astrophysical Quantities. Athlone Press
Anders E., Grevesse N., 1989, Geoch. & Cosmochim. Acta 53, 197
Arlandini C., Käppeler F., Wisshak K., et al., 1999, ApJ 525, 886
Auer L.H., Heasley J., 1976, ApJ 205, 165
Becker O., Enders K., Werth G., Dembczynski J., 1993, Phys. Rev. A48, 3546
Biehl D., 1976, Sonderdruck der Sternwarte Kiel No. 229
Brault J., Testerman L., 1972, Preliminary Kitt Peak Photoelectric Atlas. Kitt Peak Nat. Obs., Tucson
Bröstrom L., Mannervik S., Royen P., Wännström A., 1995, Phys. Scripta 51, 330
Butler K., 1999, private communication
Cameron A.G.W., 1982, Ap&SS 82, 123
Chen Y.Q., Nissen P.E., Zhao G., Zhang H.W., Benoni T., 2000 A&AS 141, 491
Crandall D.H., Taylor P.O., Dunn G.H., 1974, Phys. Rev. A10, 141
Drawin H.-W., 1961, Z. Physik 164, 513
Edvardsson B., Andersen J., Gustafsson B., et al., 1993, A&A 275, 101
Francois P., 1996, A&A 313, 229
Freiburghaus C., Rembges J.-F., Rausches T., et al., 1999, ApJ 516, 381
Fuhrmann K., 1998, A&A 338, 161
Fuhrmann K., 2000, submitted to A&A
Fuhrmann K., Pfeiffer M., Frank C., Reetz J., Gehren T., 1997, A&A 323, 909
Gilroy K.K., Sneden C., Pilachowski C.A., Cowan J.J., 1988, ApJ 327, 298
Gratton R.G., Sneden C., 1994, A&A 287, 927
Grevesse N., Noels A., Sauval A.J., 1996, ASP Conf.Ser. 99, 117
Grupp F., 1997, Diploma Thesis, Universität München
Hauge O., 1972, Solar Phys. 27, 286
Jehin E., Magain P., Neuforge C., et al., 1999, A&A 341, 241
Käppeler F., Beer H., Wisshak K., 1989, Rep. Prog. Phys. 52, 945
Komarovskii V.A., 1991, Optika i Spectroscopia 71, 559
Korn A., 1999, private communication
Krebs K., Winkler R., 1960, Z. Phys. 160, 320
Kupka F., Piskunov N., Ryabchikova T.A., Stempels H.C., Weiss W.W., 1999, A&AS 138, 119
Kurucz R.L., 1994, CD-ROM 18, 19
Kurucz R.L., Furenlid I., Brault J., Testerman L., 1984, Solar Flux Atlas from 296 to 1300 nm. Nat. Solar Obs., Sunspot, New Mexico
Magain P., 1989, A&A 209, 211
Magain P., 1995, A&A 297, 686
Magain P., Zhao G., 1993 A&A 268, L27
Martin W.C., Zalubas R., Hagan L., 1978, Atomic energy levels - The Rare Earth Elements. NSRDS-NBS 60, U.S. Gov. Print. Off., Washington., 1978
Mashonkina L.I., 2000, Astron.Rep. 44 in press
Mashonkina L.I., Gehren T., Bikmaev I.F., 1999, A&A 343, 519 (Paper I)
Massevitch A.G., Tutukov A.V., 1988, Stellar Evolution: theory and observations. Nauka, Moscow
McWilliam A., 1997, ARA&A 35, 503
McWilliam A., 1998, AJ 115, 1640
Ng Y.K., Bertelli G., 1998, A&A 329, 943
Peach G., 1967, Mem. R. Astron. Soc. 71, 13
Pfeiffer M., Frank C., Baumüller D., Fuhrmann K., Gehren T., 1998, A&AS 130, 381
Rutten R.J., 1978, Solar Phys. 56, 237

Sakhibullin N.A., 1983, Trudi Kazan gor. obs. 48, 9
Schöning T., Butler K., 1998, A&AS 128, 581
Sneden C., McWilliam A., Preston G.W., et al., 1996, ApJ 467, 819
Sneden C., Parthasarathy M., 1983, ApJ 267, 757
Steenbock W., Holweger H., 1984, A&A 130, 319
Travaglio C., Galli D., Gallino R., et al., 1999, ApJ 521, 691
Truran J.W., 1981, A&A 97, 391
Unsöld A., 1955, Physik der Sternatmosphären. 2nd edition, Springer, Berlin - Göttingen - Heidelberg
van Regemorter H., 1962, ApJ 136, 906
Wisshak K., Voss F., Käppeler F., 1996, In: Hillebrandt W., Müller E. (eds.) Proc.8th Workshop of Nuclear Astrophysics. MPA, Munich, p. 16
Woolf V.M., Tomkin J., Lambert D., 1995, ApJ 453, 660